COST Action CM1104

WG1+WG2 Workshop

Faculty of Chemistry of the Jagiellonian University, ul. Ingardena 3, 30-060, Krakow, Poland, room 30

Thursday, October 8, 2015

10:00 – 10:10	**Opening**
	SESSION 1 – Discussion leader Sergio Valeri
10:10 – 11:00	**Alessandro Fortunelli – Invited speaker** Structural and electronic properties of oxide ultrathin films via quantum approaches
11:00 – 11:30	**Coffee break**
11:30 – 11:55	**Jeppe V. Lauritsen** Atomic-scale insight into water dissociation on CoO_x/Au(111)
11:55 – 12:20	**Andrzej Kotarba** Transition metal oxides promoted with alkali - model catalysts for soot combustion
12:20 – 12:45	**Stefano Livraghi** Mechanism operating along C_2H_2 self assembly on anatase TiO_2 and its reduction
	Lunch
	SESSION 2 – Discussion leader Zbigniew Sojka
14:30 – 15:20	**Jozef Korecki – Invited speaker** Structural and electronic properties of ultrathin iron oxide films on Pt(111): from FeO to Fe_2O_3
15:20 – 15:45	**Paulina Indyka** Oxidative phase transformation of Fe_3O_4 nanoparticles during catalytic N_2O decomposition visualized by STEM/EELS at the nanoscale
15:45 – 16:10	**Joanna Gryboś** Determination of shape and size of Co_3O_4 nanocrystal catalysts from single STEM measurement
16:10 – 16:40	**Coffee break**
	SESSION 3 – Discussion leader Andrzej Kotarba
16:40 – 17:05	**Suzana Petrović** Characterization of NiO: Au nanoparticles synthesized by laser ablation in liquids
17:05 – 17:30	**Elisa Albanese** Nature of paramagnetic species in nitrogen-doped SnO_2: a combined electron paramagnetic resonance and density functional theory study
17:30 – 17:55	**Witold Piskorz** Kinetic Monte Carlo simulation of N_2O decomposition on (001)Co_3O_4
	Dinner

Friday, October 9, 2015

	SESSION 4 – Discussion leader Javier Fernandez Sanz
9:00 – 9:25	**Jacek Goniakowski** Ceria nanocrystals exposing wide (100) facets: structure and polarity Compensation
9:25 – 9:50	**Jan Ingo Flege** Growth, morphology, and interfacial structure of cerium oxide on sputter-deposited ruthenium films
9:50 – 10:15	**Paola Luches** Reversible reduction of cerium oxide ultrathin epitaxial films on Pt(111)
10:15 – 10:45	**Coffee break**
	SESSION 5 – Discussion leader Alessandro Fortunelli
10:45 – 11:20	**Monica Calatayud** Alkali incorporation in V_2O_5: an NCI analysis
11:20 – 11:40	**Marta Gałyńska** Self-interaction corrected density functional calculations of localized electron hole at Li dopant in MgO
11:40 – 12:00	**Filip Zasada** The role of the reactive oxygen species in deN_2O and $deCH_4$ reactions – DFT and catalytic TPRS and SSITKA investigations
12:00 – 12:10	**Closing**
	Lunch

Structural and Electronic Properties of Oxide Ultrathin Films via Quantum Approaches

Alessandro Fortunelli[1], Zarko Surnev[2], Falko P. Netzer[2], Teresa Cusati[3], Gianluca Fiori[3], Giuseppe Inannaccone[3], Giovanni Barcaro[1], Luca Sementa[1]

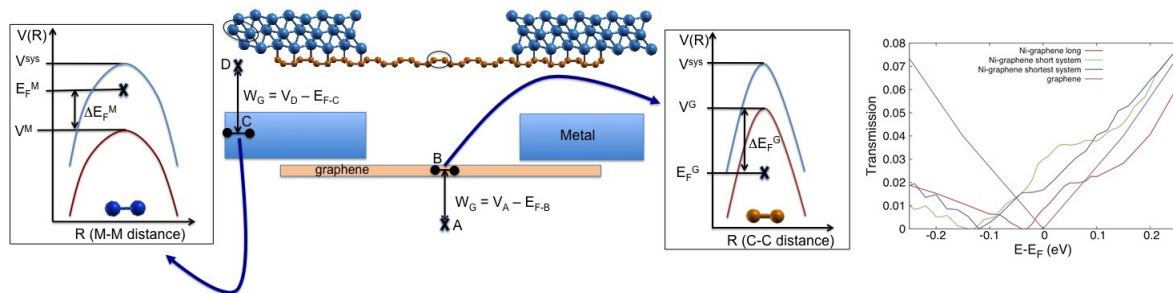[1]Consiglio Nazionale delle Ricerche, ICCOM & IPCF, v. G. Moruzzi 1 I-56124, Pisa, Italy
[2]Institute of Physics, Karl-Franzens University A-8010 Graz, Austria
[3]Dip. di Ingegneria dell'Informazione. Università di Pisa, Via G. Caruso, 16 Pisa 56122, Italy
e-mail: alessandro.fortunelli@cnr.it

An overview will be presented of our recent results in the theoretical description of the structure and properties of nanostructured oxide systems.

Starting with the structure problem, both guiding principles that can help rationalize the rich wealth of atomistically characterized films and computational tools able to conduct systematic sampling searches needed in those cases in which experimental input is lacking or insufficient will be discussed. These principles and computational tools will then be translated into the analysis of a specific system: ternary oxide ultrathin films grown on single-crystal metal surfaces. In particular, attention will be focused on metal tungstates with the general formula MWOx, in the form of CuWO4/Cu(110) [1] and FeW [2], that to the best of our knowledge are the first atomistically resolved 2D ternary oxide phases. It will be shown how an interplay of theory and experiment working in close synergy is mandatory to arrive at a correct elucidation of the structural properties of such complex materials, and how such a detailed information opens the way to a full understanding and possibly control of the response properties of such sytems.

Dielectric (oxide) ultrathin films grown on metal or semiconducting surfaces are examples of so-called 2D materials that have attracted an explosive interest in view of many applications, including electronic devices. With the goal of shedding light on electronic transport interfacial phenomena via quantum approaches, in a preliminary investigation we have studied the structure, electronic structure, and conductance between nanoribbons of several metals and graphene on which a vast literature exists to compare with. With respect to previous studies, we conducted an in-depth analysis of the charge and electrostatic potential at the metal/semiconductor junction to single out physical quantities such the work function of each fragment system, band bending and charge transfer at the interface, etc. (see the Figure below), and the consequences of the behaviour of these quantities onto conductance characteristics. We believe that our analysis sets the stage for the rationalization and prediction of transport phenomena at metal/semiconductor nanostructured contacts, including 2D oxide phases which are the subject of present on-going analysis, and that it provides the link between the knowledge accumulated on model surface science systems and technological electronic devices.

[1]   M. Denk et al. ACS Nano, **8**, 3947–3954 (2014).
[2]   Z. Surnev, F. P. Netzer, A. Fortunelli et al., (in preparation).

Atomic-scale insight into water dissociation on CoO_x/Au(111)

Jakob Fester[1], Alex Walton[1], Michal Bajdich[2], Aleksandra Vojvodic[2], **Jeppe V. Lauritsen[1]**
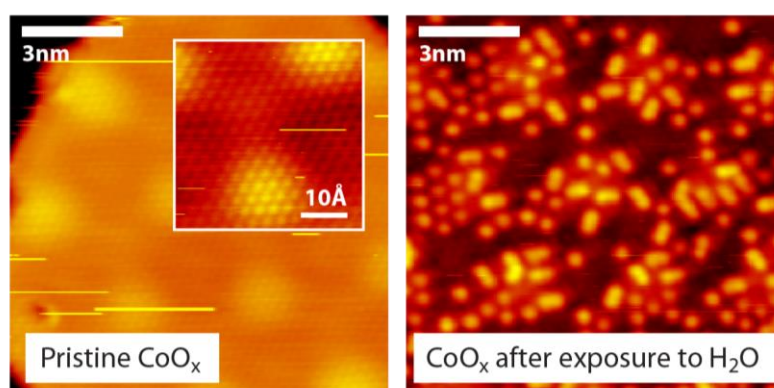[1]*Interdisciplinary Nanoscience Center Aarhus University, Aarhus, 8000, Denmark*
[2] *SUNCAT Center for Interface Science and Catalysis, SLAC National Accelerator Laboratory, 2575 San Hill Road, Menlo Park, California 94025, United States.*
email: jvang@inano.au.dk

Cobalt oxides are among the best performers as future alternative electro-catalysts for the water splitting reaction, with attractive properties in terms of stability, efficiency, abundance and low cost. However, fundamental understanding of the catalytic properties of cobalt oxides is still limited. To elucidate the fundamental structure, composition and surface chemistry of a CoO_x based catalysts, we characterize here the surface of a model catalyst consisting of CoO_x nanoislands ($0.66 < x < 2$) under ultra-high vacuum conditions by high-resolution Scanning Tunneling Microscopy (STM) and X-Ray Photoelectron and Absorption Spectroscopies (XPS and XAS) together with density functional theory.

We find that the oxygen pressure has a profound effect on the CoO_x structure, accompanied by changes in the cobalt oxidation states. The structure at low pressure is a rock-salt Co-O bilayer exposing the (111) plane with cobalt in the +2 oxidation state. However, this can be converted into a more oxygen rich stoichiometry with cobalt in the +3 state, accomplished by intercalation of an additional oxygen layer in the island/gold interface. Both structures exhibit a strong activity towards water dissociation at room temperature, leading to hydroxylation of up to 50% of the island basal plane oxygen atoms as observed in-situ by both dynamic STM movies recorded during H_2O dosing and by corresponding analysis of the hydroxyl component in the O1s core-level XPS spectrum. The reactivity towards water dissociation is shown to be directly correlated with the island edge site concentration, revealing the CoOx edges to host the most active sites. Furthermore, a detailed statistical analysis of hydroxyl mobility in STM movies reveals that the diffusion of individual basal plane hydroxyls is mediated by co-adsorbed water.

[1]   A. S. Walton, J. Fester, M. Bajdich, et al., ACS Nano 9, 2445 (2015).
[2]   B. S. Yeo and A. T. Bell, Journal of the American Chemical Society 133, 5587 (2011).

Transition metal oxides promoted with alkali - model catalysts for soot combustion

T. Jakubek, W. Kaspera, P. Legutko, P. Indyka, P. Stelmachowski, Z. Sojka, **A. Kotarba**
Faculty of Chemistry, Jagiellonian University, Ingardena 3, 30-060 Krakow, Poland
e-mail: kotarba@chemia.uj.edu.pl

The investigated materials are comprised of model 3d-metal (manganese, iron, cobalt) oxides, surface decorated or intercalated by alkali ions, which act as promoters. The guiding hypothesis consists in exploration on how the catalytic reactivity can be associated with the work function and surface/bulk status of alkali. The effect of the alkali promoters location on the surface vs. bulk (intercalation) was elucidated. The study focuses on the exploration of the key parameters governing the catalytic process: surface alkali dispersion, formation of new phases (nanostructurization), soot-catalyst interaction, topology of the soot molecular framework and the influence on the Fermi level caused by alkali doping of Mn, Fe and Co oxides. The study allows for the establishment of rational principles for designing the optimal soot oxidation catalyst based on manganese (layered birnessite KMn_4O_8 and cryptomelane KMn_8O_{16}), iron (layered $K_2Fe_{22}O_{34}$, tunneled $KFeO_2$) and cobalt (layered $KCoO_2$) oxides.

The samples were thoroughly characterized by several methods including XRD, SEM-EDX, HR-TEM/FIB, XPS, RS, BET. The electronic properties and alkali dynamics were probed by the surface work function (Kelvin Probe) and ionic conductivity measurements. The stability and surface state of alkali dopants was investigated by the Species Resolved Thermal Alkali Desorption. Catalytic activity in soot combustion (loose and tight contact) was determined by TPRS and isothermal oxidation (TG/DTA - QMS) for various catalyst/soot ratios.

Based on the obtained results an integral picture of the soot combustion process over alkali promoted catalyst was advanced and the crucial multifaceted role of alkali promotion was elucidated in detail.

Mechanism operating along C_2H_2 self assembly on anatase TiO_2 and its reduction.

Stefano Livraghi[1], Jakub Jan Biedrzycki[1], Hsin-Yi Tiffany Chen[2], Lorenzo Mino[1], Indrid Corazzari[1],Giuseppe sposto[1], Gianfranco Pacchioni[2] and Elio Giamello[1]
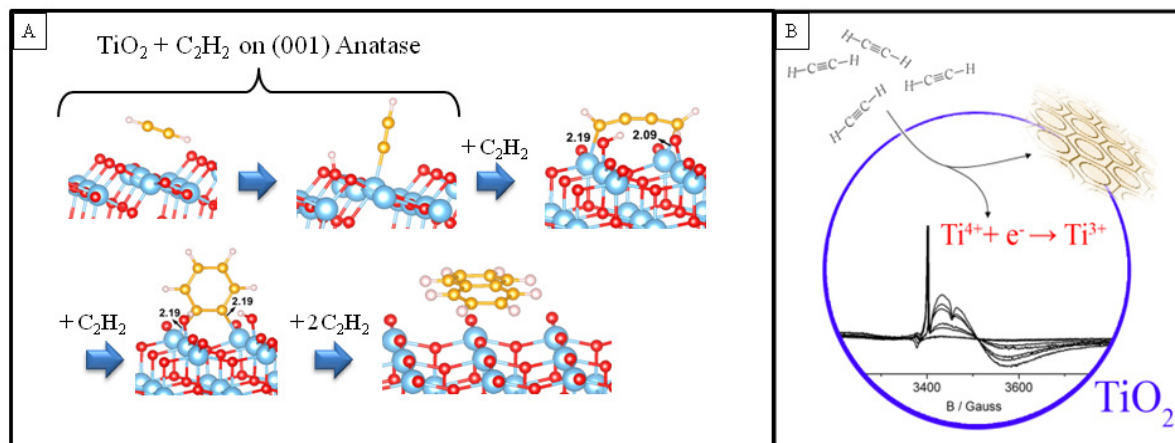[1]Dipartimento di Chimica and NIS, Università di Torino, Torino, Italy
[2] Dipartimento di Scienza dei Materiali, Università di Milano-Bicocca, Milano, Italy
Stefano.livraghi@unito.it

The interaction of acetylene with the TiO_2 surface at room temperature entails a complex set of self-assembly reactions with the formation of products having relatively high molecular weight. The C_2H_2-TiO_2 has been investigated via both experimental[1,2] and theoretical approach.[3]
C_2H_2 was adsorbed on samples submitted to different activation treatments of the surface in order to evaluate the role of the surface hydroxylation in the acetylene/TiO_2 reaction. The reaction has been monitored via Infrared (IR) and optical (UV-vis) spectroscopy, Thermogravimetric Analysis (TGA) and via continuous wave Electron Paramagnetic Resonance (CW-EPR). The experimental results show the formation of polycyclic aromatic hydrocarbons (PAH) and point towards a crucial role of the more reactive (001) facets of anatase nanoparticles. The self assembly mechanism occurring at the interface is accompanied by the formation of EPR visible Ti^{3+} centres due to electrons injection in the TiO_2 substrate.
Density functional theory (DFT) calculations show that acetylene physisorbs on the anatase (101) surface without activation of the C-H bond. On the contrary, the de-hydroxylated (001) anatase surface is very active and leads to the spontaneous splitting of the C-H bond and to the cyclo-oligomerization of the monomer.

A) Reaction profile for the cyclo-polymerization of C_2H_2 to $C_{10}H_8$ on stoichiometric (001) anatase surface.
B) Sketch representing the interaction of acetylene with the TiO_2 surface.

References

[1]   S. M. Jain, J. J. Biedrzycki, V. Maurino, A. Zecchina, L. Mino, G. Spoto J. Mater. Chem. A **2**, 12247, (2014).
[2]   J. J. Biedrzycki, S. Livraghi, I. Corazzari, L. Mino, G. Spoto, E. Giamello, Langmuir **31**, 569 (2015).
[3]   H-Y. T. Chen, S. Livraghi, E. Giamello,G. Pacchioni, *Submitted to* ChemPlusChem.

Structural and electronic properties of ultrathin iron oxide films on Pt(111): from FeO to Fe_2O_3

Józef Korecki

Jerzy Haber Institute of Catalysis and Surface Chemistry, PAS, 30-239 Kraków, Poland
AGH University of Science and Technology, 30-059 Kraków, Poland
korecki@agh.edu.pl

Different phases of iron oxides, which expose dense packed hexagonally arranged surfaces, can be epitaxially grown on Pt(111). However, the phase identification and detailed recognition of the thin film composition is non-trivial. Nuclear spectroscopies (laboratory and synchrotron based), which complement standard surface sensitive methods, show up as very helpful, as it will be presented for films of FeO, Fe_3O_4, and Fe_2O_3 stoichiometry

Bulk FeO (wüstite) has NaCl structure and is an antiferromagnet with Neel temperature approximately 200 K. By a special preparation recipe, we were able to grow metastable FeO films on Pt(111) with specific atomic and electronic structure [1]. Using nuclear inelastic scattering of synchrotron radiation, which allows to measure vibrational spectra, unusual features of the phonon density of state were revealed and discussed in terms of the dimensionality transition [2].

Contrary to FeO, film with the Fe_3O_4 stoichiometry (magnetite) preserved their structural an electronic properties down to 1 nm thickness. In particular, despite severe modifications and variation in the surface structure and composition, the Verwey transition was not suppressed. Using the combination of conversion electron Mossbauer spectroscopy and STM, the effect of the stoichiometry on the surface structure of the Fe_3O_4(111) films will be presented.

The spinel films could be converted to the corundum phase by annealing of Fe_3O_4(111) in oxygen under a moderate pressure and temperature. The resulting ultrathin α-Fe_2O_3(0001) films retain the hyperfine pattern of bulk hematite but the Morin transition is suppressed, as reported in the past [3].

References
[1] N. Spiridis et al. Phys. Rev. B 85, 075436 (2012)
[2] N. Spiridis et al. submitted, arXiv:1507.05803
[3] A. Barbier, R. Belkhou, P. Ohresser, M. Gautier-Soyer, O. Bezencenet, M. Mulazzi, M.-J. Guittet, and J.-B. Moussy, Phys. Rev. B 72, 245423 (2005)

Oxidative phase transformation of Fe_3O_4 nanoparticles during catalytic N_2O decomposition visualized by STEM/EELS at the nanoscale

Paulina Indyka, Jan Kaczmarczyk, Joanna Gryboś, J. Janas, A. Kotarba, Zbigniew Sojka
Faculty of Chemistry, Jagiellonian University, Ingardena 3, 30-060 Krakow, Poland
e-mail: paulina.indyka@uj.edu.pl

Transition metal redox oxides, particularly spinels, were found to be active catalysts for low-temperature deN_2O reaction. Depending on the electron/spin configuration and on the chemical potential of electrons, the N_2O decomposition can occur in a catalytic (Co_3O_4) or stoichiometric (Fe_3O_4) way. In the present study we explore in detail the maghemization of the Fe_3O_4 particles during N_2O decomposition by surface reactive oxygen species (ROS), using combination of EELS spectroscopy and statistical analysis techniques.

The measurements were performed with a Transmission Electron Microscope FEI Tecnai Osiris (200kV) equipped with a Gatan Quantum image filter. STEM mode with sub-nanometre probe size was used to acquire the experimental EELS data presented in Fig.1a-c.

In order to examine local changes in the phase composition and visualize the effect of oxidation of the individual Fe_3O_4 nanoparticles, as they transform toward γ-Fe_2O_3 in the course of catalytic N_2O decomposition, a spectrum image (SI) maps were acquired (Fig. 1b). From the SI maps we can get the distribution of the two iron oxides within investigated nanoparticles in nanometer-scale. We showed that magnetite/maghemite repartition can be followed by monitoring the O-K peak, since oxygen edge profiles are sensitive to the local bonding and symmetry properties of the excited oxygen anion. Spatially resolved EELS fine-structure analysis was then carried out to study the difference in the electronic structure between surface and core of the nanoparticles. We used EELSMODEL software to fit the O-K experimental spectra with a linear combination of reference O-K spectra. Fig. 1c shows extracted EELS chemical composition (color composite) maps: magnetite – red, maghemite – green. Our results revealed a clear oxidation shell at the surface region of the nanoparticles, consistent with the progressive conversion of Fe_3O_4 towards γ-Fe_2O_3 following the reaction scheme: $Fe_3O_4 + \delta/2N_2O \rightarrow Fe^{3+}[Fe^{2+}_{1-\delta}Fe^{3+}_{1+\delta}\square_{3/8\delta}]O_{4+\delta/2} + \delta/2N_2$.
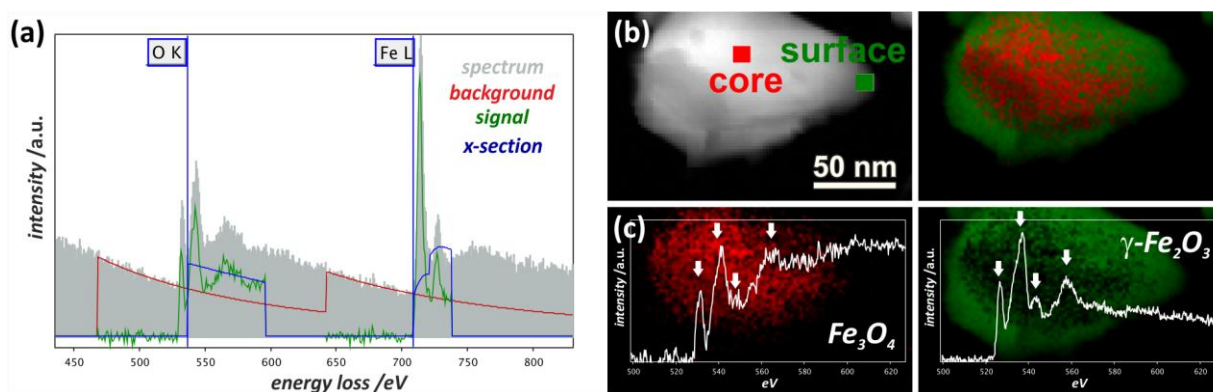

Fig. 1. Exemplary EELS spectrum displaying O-K and Fe-$L_{2,3}$ signatures (a), Spectrum Image of an iron oxide particle with indicated core and surface areas for EELS signal integration (b), oxygen K-edge fine structures 'fingerprints' overlaid with chemical composition (color composite) maps: magnetite – red, maghemite – green (c).

Determination of shape and size of Co$_3$O$_4$ nanocrystal catalysts from single STEM measurement

Joanna Grybos[1][*], Juri Barthel[2], Juan Jose Delgado Jéan[3], Filip Zasada[1], Zbigniew Sojka[1]

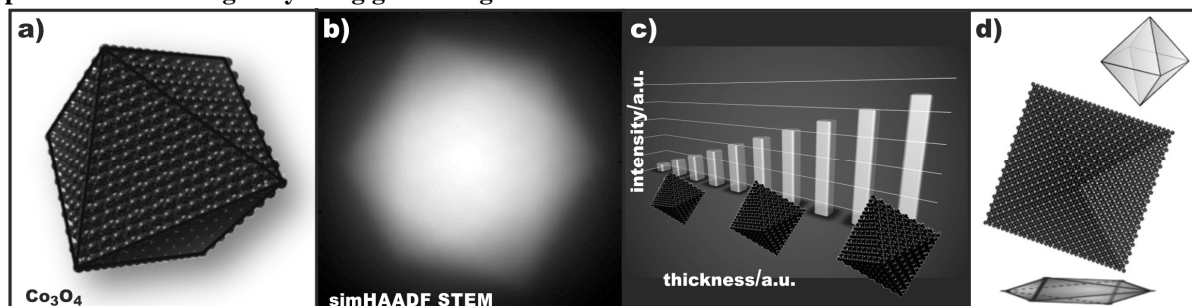[1] Jagiellonian University, Faculty of Chemistry, Ingardena 3, 30-060 Krakow

[2] Ernst Ruska-Centre, Forschungszentrum Jülich GmbH, D-52425 Jülich, Germany

[3] Inorganic Chemistry Department, University of Cadiz, Spain

[*] *grybosjo@chemia.uj.edu.pl*

By applying proper synthesis method the nanocrystals specific facets of high activity or high density of active sites may be intentionally promoted. Within this contribution, we propose a simple approach to determine the 3-dimensional size and shape of euhedral nanocrystals, using single calibrated HAADF STEM measurement [1] followed by digital processing of the image contrast. The advantage of the proposed approach arises from its simplicity concerning both the experimental and theoretical part of image processing. Being dedicated to powder catalyst samples, this method allows for efficient description of nanoparticles morphology with good statistics. To validate the method, the spinel Co$_3$O$_4$ nanocrystalline catalyst, with well-defined cubic and octahedral grains was chosen. The samples were obtained by microwave assisted hydrothermal synthesis. They were imaged in HAADF STEM mode using an intentionally broaden electron probe. The high-angle elastic scattering signal was registered as a fraction of the incident probe intensity by a calibrated detector. First step of data analysis consists of digital processing of the contrast gradient leading to the edges determination of the observed nanocrystals. For this purpose we used the convolution of the measured image with a gradient filters. For the optimal performance we have tested several filters, such as: Cannay, Prewitt, Roberts, Sobel with variable size of the kernel. Obtained edge pattern was used for retrieving the tentative shape by mean of convex hull algorithm. This step allows also for obtaining a local orientation of the nanocrystals from 2D image. The image intensity of the HAADF STEM response was calibrated against the sample thickness using numerical simulations of several randomly oriented specimens. Using the detector response calibration, the sample thickness profile was extracted from the measured grey value variations in the STEM image (on the 256 levels of grey scale). By combining retrieved local orientation of the nanocrystals and the thickness profile tentative morphology was retrieved. The definite shape was obtained using the genetic algorithm fitting. For this purpose we develop a dedicated software operating in the Matlab environment.

Fig1. a) Size and shape of nanocrystal was retrieved from digitally processed single b) HAADF STEM image. The thickness of the sample was determined by mean of the c) measurement of the grey scale variations in the HAADF STEM image. Tentative shape of the nanocrystal obtained from d) the edge pattern was converged by using genetic algorithm.

[1] J. M. LeBeau, S. D. Findlay, L. J. Allen, S. Stemmer Nano Lett 10 (2010) 4405

Characterization of NiO:Au nanoparticles synthesized by laser ablation in liquids

Suzana Petrović[1], B. Salatić[2], D.Peruško[1] J. Kovač[3], G. Dražić[4] and B. Jelenković[2]

(1) *Institute of Nuclear Science—Vinča, University of Belgrade, POB 522, 11001 Belgrade, Serbia*

(2) *Institute of Physics Belgrade, University of Belgrade, Pregrevica 118, 11080 Belgrade, Serbia*

(3) *Jožef Stefan Institute, Jamova 39, 1000 Ljubljana, Slovenia*

(4) *National Institute of Chemistry, Hajdrihova 19, Ljubljana, Slovenia*

Contact: S. Petrović (spetro@vinca.rs)

Abstract. The unique optical and electric properties have been researched and utilized in high technology applications such as organic photovoltaics, sensory probes, therapeutic agents, drug delivery in biological and medical applications, electronic conductors and catalysis [1]. Bimetallic NiAu nanoparticles can be potentially important system as effective catalyst in a few catalytic reactions and in the biotechnology as a magnetic targeting carrier [2]. The higher catalytic activity of the NiAu NPs than the pure Ni and Au NPs can issue electronic charged transfer from Ni atoms to Au atoms, generating the differently charged Ni and Au, which can act as catalytically active sites [3]. Also, noble metallic NPs embedded between metal-oxide nanocomposites, serving as nanoelectrodes, reduce the resistivity of electrochemical solid-state gas sensors and improve performance of a sensing device. Recently, it has been found that the hydrogen sensors composed from Au nanoparticles embedded in NiO film, achieve sensing of hydrogen concentration as low as 5 ppm, operating in the $100 - 160$ ^oC temperature range.

Complex NiO:Au nanoparticles were formed by laser ablation of Ni target immersed in the colloidal gold solution. Effect of laser pulse duration on size and composition of nanoparticles was investigated by ablating the target with two Nd:YAG lasers at 1064 nm, operating with different pulse durations, 150 ps and 20 ns. Repetition rate of pulses (10 Hz), energy per pulse (10 mJ) of two lasers were kept constant during the synthesis of nanoparticles. Stronger ablation of the Ni target and subsequient synthesis of nanoparticles is achieved with picosecond pulses, compared to the nanoparticles production with nanosecond pulses, because the former ablation induces activation of different reactions between species in the colloidal solution. Shape, size and composition of the synthesized nanopraticles were found to correlate with the concentration of Ni species in the colloidal solution. Higher Ni concentration leads to formation of larger NiAu nanoparticles in form of solid solution. Smaller nanoparticles with lower Ni concentration in the colloidal solution were achieved by their synthesis during nanosecond pulses, when the obtained distribution of composition corresponds to the NiO matrix with incorporated golden nanoparticles. The results also demonstrate that the formation of bimetallic NiAu and complex NiO:Au nanoparticles were possible by means of laser ablation in liquids.

REFERENCES

[1] S. Duan, R. Wang, , *Progress in Natural Science: Materials International*, **23**, (2013) 113-126.
[2] E. Xiu-tian-feng, Y. Zhang, J.J. Zou , X. Zhang, L. Wang, , *Materials Letters* **118**, (2014) 196–199
[3] F. Mafune, T. Okamoto, M. Ito, *Chemical Physics Letters* **591**, (2014) 193-196

Nature of Paramagnetic Species in Nitrogen-doped SnO$_2$: A Combined Electron Paramagnetic Resonance and Density Functional Theory Study

Elisa Albanese,[†] Cristiana Di Valentin, [†] Gianfranco Pacchioni, [†] Frédéric Sauvage,[§‡] Stefano Livraghi[‡] and Elio Giamello[‡]

[†] Dipartimento di Scienza dei Materiali, Università Milano Bicocca, via R. Cozzi, 55 – 20125 Milano, Italy
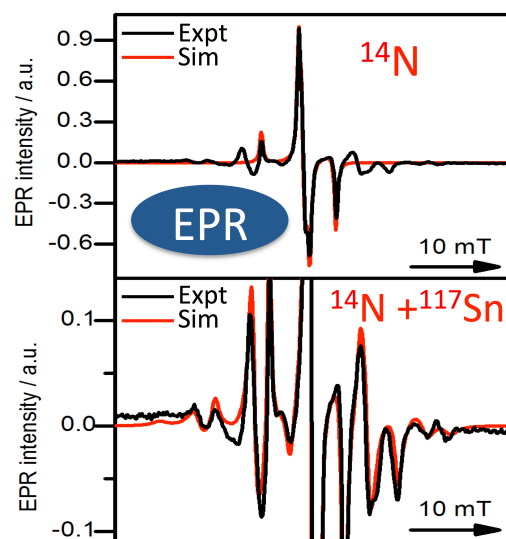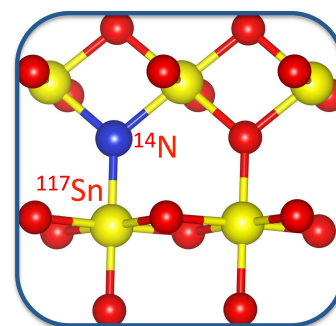[§] Laboratoire de Réactivité et Chimie des Solides (CNRS UMR 7314), Université de Picardie Jules Verne, 33 rue Saint-Leu, 80039 Amiens Cedex, France
[‡] Dipartimento di Chimica and NIS, Università di Torino, Via P. Giuria 7, I - 10125 Torino, Italy

SnO$_2$ is a multifunctional oxide semiconductor finding application in several fields. In particular, with a bandgap of 3.6 eV, SnO$_2$ is a promising material for ultraviolet light emitting diodes (LED) and photodetectors. In order to extend the photocatalytic activity towards the visible range various strategies have been explored, such as doping, nanostructuring, surface modification or functionalization. The inclusion of nitrogen dopant into the SnO$_2$ lattice is a credible approach to tune the absorption properties, either via bandgap narrowing or by introducing new energy states into the gap. [1] In this work, a combination of electron paramagnetic resonance (EPR) spectra and density functional theory (DFT) calculations is used to characterize the paramagnetic species in rutile N-doped SnO$_2$ samples synthesized by wet chemistry methods. In particular, the nature of paramagnetic N species, substitutional and interstitial, and their effect on the electronic structure are investigated. Complex EPR spectra generated by the interaction of the unpaired electron with N and Sn nuclei have been accurately simulated to obtain the EPR properties (g and A tensors).

The calculations were carried out by means of hybrid DFT functional (B3LYP) as implemented in CRYSTAL14 code. All electron basis sets are used for all the atoms.

The results suggest that the N dopants form a rather symmetric structure with three magnetically equivalent or nearly equivalent Sn atoms surrounding the N impurity. After a careful assessment of an all electron basis set for Sn atoms, realistic models of substitutional and interstitial N-doped SnO$_2$ structures have been designed, and the corresponding hyperfine coupling constants (hpcc) computed. The comparison between computed and measured hpcc values leads to the assignment of the paramagnetic centres in N-SnO$_2$ to substitutional N dopants that take the position of the O atoms in the lattice. The DFT calculations finally suggest the N impurities induce the formation of localized empty states (electron holes) in the intra bandgap, as expected.[2,3]

[1] Pan, S. S.; Ye, C.; Teng, X. M.; Fan, H. T.; Li, G. H. Preparation and characterization of nitrogen-incorporated SnO$_2$ films. *Appl. Phys. A: Mater. Sci. Process* 2006, *85*, 21-24.
[2] Long, R.; English, N. J. Density functional theory description of the mechanism of ferromagnetism in nitrogen-doped SnO$_2$. *Physics Letters A* 2009, *374*, 319-322.
[3] Di Valentin, C.; Finazzi, E.; Pacchioni, G.; Selloni, A.; Livraghi, S.; Paganini, M. C.; Giamello, E. N-doped TiO$_2$: theory and experiment. *Chemical Physics* 2007, *339*, 44-56.

Kinetic Monte Carlo simulation of N2O decomposition on (001)Co$_3$O$_4$

Witold Piskorz, Filip Zasada, Zbigniew Sojka

Faculty of Chemistry, Jagiellonian University, Ingardena 3, 30-060 Kraków, Poland

wpiskorz@chemia.uj.edu.pl

The kMC simulation was carried out for the elementary steps network of catalytic decomposition of N$_2$O over the (001) face of Co$_3$O$_4$ in the presence of co-adsorbing dioxygen and water. All surface octahedral cobalt (Co^{oct}), tetrahedral cobalt (Co^{tetr}), and oxygen sites were taken into account (see Figure 1; the conceivable pairs are rendered by sticks).
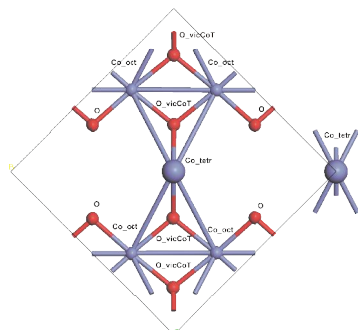
The activation free energies were calculated based on the DFT GGA-PW91 level of theory, and the harmonic vibrational analysis. The dissociative adsorption was calculated as the sequence of simple adsorption ($k = p$ (kT)/h exp($-E_{ads}$/kT)), and the dissociation of adsorbed species ($k = $ (kT)/h exp($-E_{diss}$/kT)). The NN–O bond cleavage products, O$_{ads}$, would subsequently undergo two mechanisms of two-center recombination towards O$_{2(g)}$, either the Hinshelwood-Langmuir or the Elay-Rideal mechanisms. The O$_{ads}$ can also be formed by readsorption of O$_{2(g)}$.

All conceivable modes of O$_{ads}$ diffusion were calculated and implemented in kMC for all pairs of adjacent surface ions (satisfying periodic boundary conditions) or for all single ions for two-centre and one-centre reaction steps, respectively. The following elementary acts were taken into account:

N$_2$O$_{(g)}$ + Co$_{(oct)}$ $\rightarrow$ N$_{2(g)}$ + O$^-$/Co$^{\bullet}_{(oct)}$	electron transfer activation of N$_2$O
O$^-$/Co$^{\bullet}_{(oct)}$ + Co$_{(oct)}$ $\leftrightarrow$ Co$_{(oct)}$ + O$^-$/Co$^{\bullet}_{(oct)}$	diffusion channel 1: O$^-$ diffusion
O$_2^{2-}$ $_{(surf)}$ + O^{2-} $_{(surf)}$ $\leftrightarrow$ O^{2-} $_{(surf)}$ + O$_2^{2-}$ $_{(surf)}$	diffusion channel 2: O$_2^{2-}$ $_{(surf)}$ diffusion
O$^-$/Co$^{\bullet}_{(oct)}$ + O^{2-} $_{(surf)}$ $\leftrightarrow$ Co$_{(oct)}$ + O$_2^{2-}$ $_{(surf)}$	diffusion channel switch
O$_2^{2-}$ $_{(surf)}$ + O^{2-} $_{(surf)}$ $\rightarrow$ 2 O^{2-} $_{(surf)}$ + O$_{2(g)}$	anionic channel of O$_2$ recombination
O$^-$/Co$^{\bullet}_{(oct)}$ + O$^-$/Co$^{\bullet}_{(oct)}$ $\rightarrow$ 2 Co$_{(oct)}$ + O$_{2(g)}$	cationic channel of O$_2$ recombination
O$^-$/Co$^{\bullet}_{(oct)}$ + O$_2^{2-}$ $_{(surf)}$ $\rightarrow$ Co$_{(oct)}$ + O^{2-} $_{(surf)}$ + O$_{2(g)}$	mixed channel of O$_2$ recombination
O$_2^{2-}$ $_{(surf)}$ + N$_2$O$_{(g)}$ $\rightarrow$ N$_{2(g)}$ + O$_{2(g)}$ + O^{2-} $_{(surf)}$	Elay-Rideal O$_2$ recombination
O$_{2(g)}$ + Co$_{(oct)}$ $\rightarrow$ O$_2^-$/Co$^{\bullet}_{(oct)}$	O$_2$ readsorption on Co$_{(oct)}$

The role of water, either associatively or dissociatively adsorbed (yielding Co$_{surf}$–OH and O$_{surf}$–H), was limited to blocking the adsorption sites and thus hindering the adsorption of N$_2$O and the diffusion of O$_{ads}$.

Ceria Nanocrystals Exposing Wide (100) Facets: Structure and Polarity Compensation

Yi Pan[1], Niklas Nilius[1,2], Christian Stiehler[1], Hans-Joachim Freund[1], **Jacek Goniakowski**[3], and Claudine Noguera[3]

[1] Fritz-Haber-Institut der Max-Planck-Gesellschaft, D-14195 Berlin , Germany
[2] Carl von Ossietzky Universität Oldenburg Institut für Physik, D-26111 Oldenburg , Germany
[3] Institut des Nanosciences de Paris, CNRS & Univ. Paris 06, F-75005 Paris , France

nilius@fhi-berlin.mpg.de, jacek.goniakowski@insp.jussieu.fr

We discuss the structural and morphological properties of ceria crystallites that develop from compact CeO_2(111) films grown on Ru(0001) by annealing in an oxygen-poor environment. With increasing temperature, the particles undergo a distinct shape evolution that finally leads to crystallites exposing wide (100) facets. The atomic structure of the (100) termination is determined by a combination of high-resolution scanning tunneling microscopy and density functional theory. Two surface reconstructions are identified, both are compatible with the need to compensate for the intrinsic dipole of the (100) plane and with a substantial reduction of the oxide material. While the main (2×2) phase is composed of pyramidal CeO_4 units, similar to the Wolf reconstruction, an oxygen termination has been determined for a c(2×2) minority phase. Both structures are further stabilized by oxygen removal from the stoichiometric surfaces. Our study provides insights into the rarely explored (100) surface of ceria, which can be considered as model system for studying chemical processes on the polar termination of reducible oxides.

[1] Y. Pan, N. Nilius, C. Stiehler, H.-J. Freund, J. Goniakowski, and C. Noguera, Adv. Mater. Interfaces, **1**, 1400404 (2014).

Growth, morphology, and interfacial structure of cerium oxide on sputter-deposited ruthenium films

Marc Sauerbrey, Jan Höcker, Jens Falta, and **Jan Ingo Flege**
Institute of Solid State Physics, University of Bremen, Bremen, Germany

flege@ifp.uni-bremen.de

Low-energy electron microscopy was used to follow the growth of cerium oxide by reactive molecular beam epitaxy on sputter-deposited ruthenium(0001) films of about 100 nm thickness that were previously evaporated onto Al_2O_3 substrates by magnetron sputtering. Structural analysis prior to ceria deposition confirms the flatness, smoothness, and high crystallinity of the ruthenium films after careful thermal annealing.

Sequentially, ceria growth was performed at 900°C and monitored *in situ* using low-energy electron microscopy (LEEM), providing detailed information into the growth and subsequent ripening processes of the ceria islands as well as the step edge structures on top. The resulting nanoparticles and microparticles are single crystalline and exhibit (111) or (100) top facets depending on the local morphology of the substrate. Ex situ atomic force microscopy reveals that the ceria(111) islands are atomically flat and form equilateral triangles with steep side facets. Complementary characterization by high-resolution transmission electron microscopy confirms the carpet-like growth behavior and shows the ceria/Ru interface to be abrupt and well ordered.

Reversible reduction of cerium oxide ultrathin epitaxial films on Pt(111)

P. Luches[1], G. Gasperi[1,2], L. Amidani[3,4], F. Benedetti[1,2], F. Boscherini[3], S. Valeri[1,2]

[1]Istituto Nanoscienze, Consiglio Nazionale delle Ricerche, Modena, Italy
[2]Dipartimento di Scienze Fisiche Matematiche e Informatiche, Università degli studi di Modena e Reggio Emilia, Modena, Italy
[3] Dipartimento di Fisica e Astronomia, Università di Bologna, Bologna, Italy
[4] ESRF, F-38043 Grenoble, France

e-mail: paola.luches@unimore.it

We have studied the modifications of morphology, atomic and electronic structure of ultrathin epitaxial cerium oxide films supported on Pt(111) during reduction and re-oxidation induced by thermal cycles in vacuum and oxygen atmosphere. The oxidation state is evaluated by XPS, while the evolution in surface structure and morphology are investigated by LEED and STM, respectively [1]. Different surface reconstructions appear in the LEED at increasing degrees of reduction, and they are accompanied by non negligible modifications in morphology. [1] Based on these results, we have performed a study of the modifications of the electronic structure of the films during reduction/oxidation treatments by high-resolution XANES measurements at the Ce L_3-edge. The evolution of the empty state structure close to the Fermi level and of the $4f$ electronic configuration during reduction was found to be much more significant on an ultrathin film than on a thicker one.

[1] P. Luches, F. Pagliuca, S. Valeri, Phys. Chem. Chem. Phys. **16**, 18848 (2014).

Alkali incorporation in V_2O_5: an NCI analysis

V. Riffet[1,2], J. Contreras-Garcia[1,2], J. Carrasco[3], **M. Calatayud[1,2,4]**

[1] Sorbonne Universités, UPMC Univ Paris 06, UMR 7616, Laboratoire de Chimie Théorique, F-75005, Paris, France
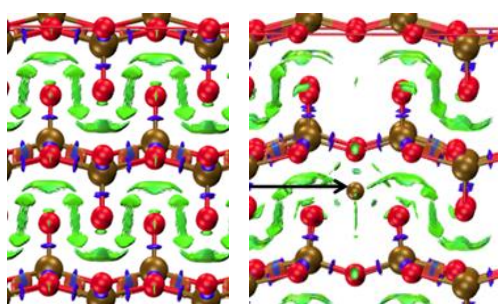[2] CNRS, UMR 7616, Laboratoire de Chimie Théorique, F-75005, Paris, France
[3] CIC energigune, Albert Einstein 48, 01510 Miñano, Alava, Spain
[4] Institut Universitaire de France, France

calatayu@lct.jussieu.fr

The interaction of V_2O_5 with alkali ions is important for many technological applications such as heterogeneous catalysis (1) and batteries (2). Understanding the nature and the extent of the interaction between ions and matrix is necessary to unravel the mechanisms of stabilization of the system.

Bulk vanadia structure is composed of layers stacked in the (001) direction, the cohesion of the crystal is ensured by Van der Waals forces. The addition of alkali atoms in the bulk material takes place in the interlayer positions thus altering the forces balance. Recently, the thermodynamics and kinetics of alkali and alkaline-earth doped alpha-vanadia has been addressed by some of us, showing that the Van der Waals interactions are responsible for a stabilization of the ions in the matrix, increasing the activation energy needed for diffusion(3). In the present work we aim at describing and analyzing the interactions in the alkali-vanadia materials through the use of non-covalent interactions index (NCI), complementing previous works that characterize chemically active sites in vanadia-based materials(4). NCI, based on the reduced electron density gradient, has proven to be able to reveal weak interactions, enabling the characterization and visualization of both stabilizing (hydrogen bonds, van der Waals) and destabilizing (steric clashes) interactions(5). We will show that the NCI analysis is well suited for the study of solid systems and captures both weak (dispersive interlayer) and strong

(ionic V-O and alkali-O) interactions. Moreover, it accounts for the fine bonding structure, revealing the presence of V^{4+} sites formed when alkali ionize, as well as unexpected stabilizing cycle interactions. It is therefore a very useful tool for the analysis of bonding in layered materials.

Figure: NCI isosurface plot in the vanadia bulk structure (left) and in the presence of Na (right, arrow indicates Na). The presence of alkali atoms modifies the interactions between layers (green).

References
(1) Zhao, Z. et al. *Topics in Catal.* **2006**, *38*, 309; Calatayud, M. and Minot, C. *J. Phys. Chem. C* **2007**, *111*, 6411; Lewandowska, A. E. et al. *Catal. Today* **2008**, *139*, 209.
(2) Whittingham, M. S. *Chem. Rev.* **2004**, *104*, 4271-4302; Tarascon, J. M. et al. *Nature* **2001**, *414*, 359.
(3) Carrasco, J. *J. Phys. Chem. C* **2014**, *118*, 19599.
(4) Calatayud, M. et al. *Chem. Phys. Lett.* **2001**, *333*, 493 *ibid* **2008**, *456*, 59.
(5) Johnson, E. R. et al. *J. Am. Chem. Soc.* **2010**, *132*, 6498; Contreras-Garcia, J. et al. *J. Chem. Theory Comput.* **2011**, *7*, 625.

Self-interaction corrected density functional calculations of localized electron hole at Li dopant in MgO

Marta Gałyńska, Elvar Jónsson, John C. Carey, Michael Nolan and Hannes Jónsson

Applied Physics Dpt., Aalto University, Espoo, Finland
Tyndall National Institute, Cork, Ireland
Faculty of Physical Sciences, University of Iceland, Reykjavík, Iceland
marta.galynska@gmail.com

Abstract:
Theoretical calculations of the localized hole formed near a Li-atom dopant in MgO are presented. This system has become an important catalyst for methane activation and there have been several experimental and theoretical studies to determine the reaction mechanism. We find that commonly used DFT functionals such as generalized gradient approximation as well as commonly used hybrid functionals, such as HSE06, fail to stabilize the localized hole due to the self-interaction error inherent in Kohn-Sham density functionals. This is analogous to the extensively documented case of Al-atom dopant in SiO_2 [1,2,3]. The present results show that variational, self-consistent calculations using the Perdew-Zunger self-interaction correction [3,4] involving complex optimal orbitals [5] can reproduce well the experimentally deduced lengthening of a single Li-O bond to the O-atom where the hole resides as well as the energy of the defect state (calculated to be 2.1 eV above the valence band edge) and the size of the band gap (8.0 eV both measured and calculated). Results obtained by varying the amount of exact exchange in the HSE functional form, and DFT+U will also be presented.
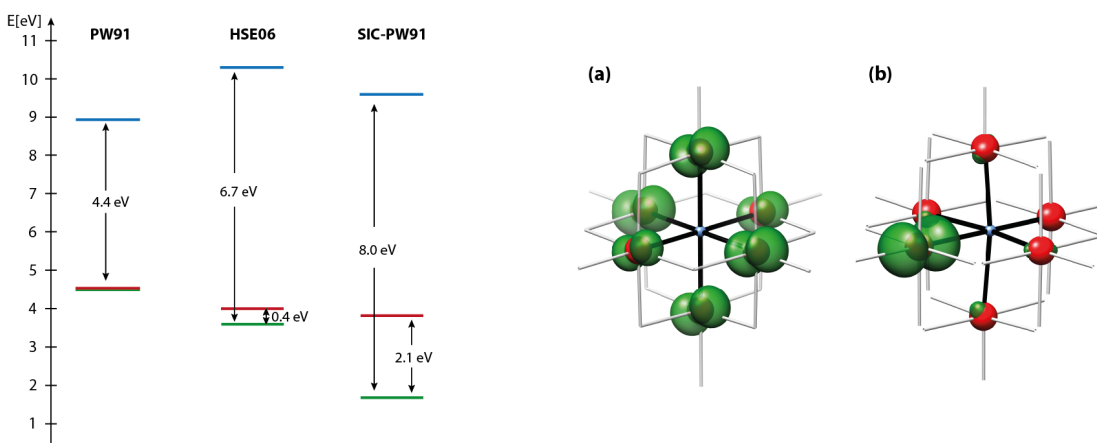
Fig. Left: Energy diagram comparing PW91, HSE06 and PZ-SIC results for Li-MgO. Right: Spin density calculated using (a) HSE06 and (b) PZ-SIC applied to the PW91 functional.

References:
[1] G.Pacchioni, *J. Chem. Phys.* **128**, 182505(2008); G.Pacchioni et al. *Phys. Rev. B* **63**, 054102 (2000).
[2] J. Lægsgaard and K. Stokbro, Phys. Rev. Letters **86**, 2834 (2001).
[3] H. Gudmundsdóttir, E. Ö. Jónsson and H. Jónsson, New Journal of Physics **17**, 083006 (2015).
[3] J. P. Perdew and A. Zunger, *Phys. Rev. B* **23**, 5048 (1981).
[4] P. Klüpfel, S. Klüpfel, K. Tsemekhman, and H. Jónsson, *Lect. Notes in Comp. Sci.* **7134**, 23 (2012).
[5] S. Klüpfel, P. J. Klüpfel and H. Jónsson, *Phys. Rev. A* 84, 050501 (2011); *J. Chem. Phys.* 137, 124102 (2012).

The Role of the Reactive Oxygen Species in deN_2O and $deCH_4$ reactions – DFT and catalytic TPRS and SSITKA investigations

F. Zasada, J. Janas, W. Piskorz, J. Kaczmarczyk, A. Kotarba, Z. Sojka
Faculty of Chemistry, Jagiellonian University, ul. Ingardena 3, 30-060 Krakow, Poland
e-mail address of corresponding author: zasada@chemia.uj.edu.pl

Cobalt (II,III) spinel is an excellent redox-tunable model catalytic material of widespread fundamental and practical interest, which has been found to be active in methane oxidation and in the low temperature decomposition of N_2O. A governing factor of its high catalytic performance can be attributed to presence of various surface reactive oxygen species (ROS) and to facile formation of oxygen vacancies. The ROS adspecies are produced by associative and dissociative adsorption modes of dioxygen, and are suggested to play a key role in the deN$_2$O and low temperature CH_4 oxidation reaction. At higher temperatures oxygen vacancies are also involved in the CH_4 combustion (the Mars-van Krevelen redox cycle).
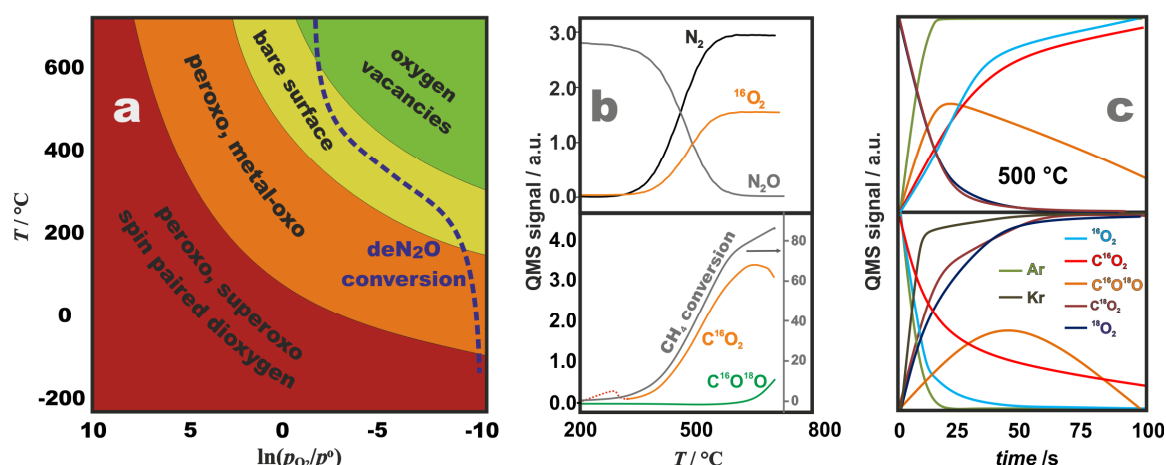

Figure 1: Atomistic thermodynamics surface state diagram of cobalt spinel (100) surface (a) together with deN$_2$O and deCH$_4$ TPSR profiles (b) and SSITKA results (c).

In this work we present DFT+U based atomistic thermodynamics surface state diagram (Figure 1a) for the (100) facet of cobalt spinel for wide range of oxygen pressures and temperature. It is shown that for oxygen pressures of typical catalytic reactions, three principal states of the spinel surface correspond to oxygen adsorption (ROS region, $T < 350 \div 400\,°C$), bare surface region ($350 \div 400\,°C$ to $550 \div 700\,°C$) and oxygen release region ($T > 550$-$700\,°C$). Superoxo, peroxo and metal-oxo species are produced by surface to oxygen electron transfer involving remote donor centers constituted by octahedral Co^O_{5c} sites. N_2O decomposition (Figure 1b, top) were used to probe recombination of surface ROS on bare surface, whereas CH_4 oxidation (Figure 1b, bottom) to examine their reactivity. It is shown that the C–H bond in methane is activated by cobalt-oxo $[Co^T_{2c}\text{-}O^+]$ species. The reaction starts at $350\,°C$ following Eley-Rideal scheme, and above $600\,°C$ evolves toward the Mars-van Krevelen mechanism due to gradual engagement of lattice O_{3c} oxygen, as revealed in SSITKA experiments (Figure 1c) using ^{18}O isotopically labelled dioxygen.